32. A. N. Kapanidis *et al.*, *Science* **314**, 1144 (2006).
33. M. Gotte, G. Maier, H. J. Gross, H. Heumann, *J. Biol. Chem.* **273**, 10139 (1998).
34. H. Huang, R. Chopra, G. L. Verdine, S. C. Harrison, *Science* **282**, 1669 (1998).
35. J. Ren *et al.*, *Nat. Struct. Biol.* **2**, 293 (1995).
36. Y. Quan, C. Liang, P. Inouye, M. A. Wainberg, *Nucleic Acids Res.* **26**, 5692 (1998).
37. L. Ratner *et al.*, *Nature* **313**, 277 (1985).
38. P. H. von Hippel, O. G. Berg, *J. Biol. Chem.* **264**, 675 (1989).
39. H. Kabata *et al.*, *Science* **262**, 1561 (1993).
40. M. Guthold *et al.*, *Biophys. J.* **77**, 2284 (1999).
41. P. C. Blainey, A. M. van Oijen, A. Banerjee, G. L. Verdine, X. S. Xie, *Proc. Natl. Acad. Sci. U.S.A.* **103**, 5752 (2006).
42. J. Elf, G. W. Li, X. S. Xie, *Science* **316**, 1191 (2007).
43. K. B. Hall, L. W. McLaughlin, *Biochemistry* **30**, 10606 (1991).
44. N. Sugimoto, S. Nakano, M. Yoneyama, K. Honda, *Nucleic Acids Res.* **24**, 4501 (1996).
45. G. J. Klarmann, C. A. Schauber, B. D. Preston, *J. Biol. Chem.* **268**, 9793 (1993).

46. This work is supported in part by NIH (GM 068518 to X.Z.) and the Intramural Research Program of the Center for Cancer Research, National Cancer Institute (to S.F.J.L.G.). X.Z. is a Howard Hughes Medical Institute investigator. E.A.A. is a Jane Coffin Childs postdoctoral fellow. Nevirapine was provided through the AIDS Research and Reference Reagent Program of NIH.

Supporting Online Material

www.sciencemag.org/cgi/content/full/322/5904/1092/DC1
Materials and Methods
Figs. S1 to S12
References

11 July 2008; accepted 24 September 2008
10.1126/science.1163108

Batf3 Deficiency Reveals a Critical Role for CD8α$^+$ Dendritic Cells in Cytotoxic T Cell Immunity

Kai Hildner,[1,2] Brian T. Edelson,[1] Whitney E. Purtha,[3] Mark Diamond,[1] Hirokazu Matsushita,[1] Masako Kohyama,[1,2] Boris Calderon,[1] Barbara U. Schraml,[1] Emil R. Unanue,[1] Michael S. Diamond,[1,3] Robert D. Schreiber,[1] Theresa L. Murphy,[1] Kenneth M. Murphy[1,2]*

Although in vitro observations suggest that cross-presentation of antigens is mediated primarily by CD8α$^+$ dendritic cells, in vivo analysis has been hampered by the lack of systems that selectively eliminate this cell lineage. We show that deletion of the transcription factor *Batf3* ablated development of CD8α$^+$ dendritic cells, allowing us to examine their role in immunity in vivo. Dendritic cells from *Batf3*$^{-/-}$ mice were defective in cross-presentation, and *Batf3*$^{-/-}$ mice lacked virus-specific CD8$^+$ T cell responses to West Nile virus. Importantly, rejection of highly immunogenic syngeneic tumors was impaired in *Batf3*$^{-/-}$ mice. These results suggest an important role for CD8α$^+$ dendritic cells and cross-presentation in responses to viruses and in tumor rejection.

During antigen cross-presentation (*1*), antigens generated in one cell are presented by major histocompatibility complex (MHC) class I molecules of a second cell. It remains unclear whether all antigen presenting cells (APCs) use cross-presentation and whether this pathway plays a role in immune responses in vivo (*2*). Dendritic cells (DCs) are a heterogeneous group of APCs with two major subsets, plasmacytoid dendritic cells (pDCs) and conventional CD11c$^+$ dendritic cells (cDCs) (*3*). Subsets of cDCs include CD8α$^+$, CD4$^+$, and CD8α$^-$CD4$^-$ populations that may exert distinct functions in immune responses. Evidence has suggested that CD8α$^+$ cDCs are important for cross-presentation during infections but has its basis in ex vivo analysis (*4*–*6*) or in vitro antigen loading (*7*). Evidence both for and against a role for cross-presentation in responses against tumors has been reported (*8*–*10*).

Attempts have been made to study the in vivo role of DCs by selective depletion. Diphtheria toxin treatment can deplete all CD11c^{hi} cells in one transgenic mouse model (*11*) but affects splenic macrophages and activated CD8$^+$ T cells (*12*). Gene targeting of transcription factors (e.g., *Irf2*, *Irf4*, *Irf8*, *Stat3*, and *Id2*) has caused broad defects in several DC subsets, T cells, and macrophages (*13*). To identify genes regulating DC development, we performed global gene expression analysis across many tissues and immune cells (fig. S1A). *Batf3* (also known as *Jun dimerization protein p21SNFT*) (*14*) was highly expressed in cDCs, with low to absent expression in other immune cells and nonimmune tissues. Thus, we generated *Batf3*$^{-/-}$ mice that lack expression of the Batf3 protein (fig. S1, B to D).

In spleens of *Batf3*$^{-/-}$ mice, we found a selective loss of CD8α$^+$ cDCs, without abnormalities in other hematopoietic cell types or architecture (Fig. 1 and figs. S2 to S14). CD8α$^+$ cDCs coexpress DEC205, CD24, and low levels of CD11b (*3*, *15*). *Batf3*$^{-/-}$ mice lacked splenic CD11c^{hi}CD8α$^+$DEC205$^+$ cells (Fig. 1A), showed a loss of CD11c^{hi}CD11b^{dull} cells and CD11c^{hi}CD8α$^+$CD24$^+$ cells (Fig. 1B), but had normal populations of CD4$^+$ and CD8α$^-$CD4$^-$ cDC subsets (Fig. 1B). Lymph nodes and thymi of *Batf3*$^{-/-}$ mice lacked CD8α$^+$ DCs but had normal distributions of CD8α$^-$CD11c$^+$ cells (Fig. 1C). DEC205^{int} and DEC205^{hi} DCs were present in lymph nodes draining the skin of *Batf3*$^{-/-}$ mice (Fig. 1C) and showed normal migration from skin to lymph node after topical application of fluorescein-5-isothiocyanate (fig. S3A). *Batf3*$^{-/-}$ mice had normal development of pDCs (CD11c^{int}CD11b$^-$B220$^+$) (fig. S3B), interstitial DCs of pancreatic islets (CD11c$^+$CD8α$^-$) (fig. S3, C and D), monocytes, neutrophils (fig. S3E), and SIGN-R1$^+$ marginal zone and MOMA-1$^+$ metallophilic macrophages (Fig. 2A). CD8α$^+$ cDCs developed normally in heterozygous *Batf3*$^{+/-}$ mice (fig. S4A) and were absent in *Rag2*$^{-/-}$ *Batf3*$^{-/-}$ mice (fig. S4B).

This loss of CD8α$^+$ cDCs could result from a cell-autonomous hematopoietic defect or a cell-extrinsic requirement for *Batf3*. To distinguish these possibilities, we generated chimeras in which CD45.2$^+$ *Batf3*$^{+/+}$ or CD45.2$^+$ *Batf3*$^{-/-}$ bone marrow (BM) was transplanted into lethally irradiated CD45.1$^+$CD45.2$^+$ recipients (Fig. 2B). Upon reconstitution (fig. S5A), we found CD8α$^+$ cDCs developed only from *Batf3*$^{+/+}$ donor BM cell (Fig. 2B), indicating a cell-intrinsic hematopoietic defect in *Batf3*$^{-/-}$ mice.

Treatment of mice with fms-like tyrosine kinase 3 (flt3) ligand–Fc (FL-Fc) increased the numbers of CD8α$^+$ cDCs, CD8α$^-$ cDCs, and pDCs in *Batf3*$^{+/+}$ mice but failed to increase the number of CD8α$^+$ cDCs in *Batf3*$^{-/-}$ mice (Fig. 2C). In vitro culture of BM with FL generates cell populations corresponding to pDCs (CD11c$^+$CD45RA$^+$) and cDCs (CD11c$^+$CD45RA$^-$) (*3*, *16*) (Fig. 2D). These in vitro–derived cDCs do not express CD8α or CD4 but contain a CD24$^+$Sirp-α$^{lo\text{-}int}$ population corresponding to CD8α$^+$ cDC (*16*). *Batf3*$^{+/+}$ or *Batf3*$^{-/-}$ BM cells treated with FL produced similar ratios of pDCs and cDCs (Fig. 2D and fig. S5B). However, *Batf3*$^{-/-}$ BM generated far fewer CD24$^+$ Sirp-α$^-$ cells compared with *Batf3*$^{+/+}$ BM (Fig. 2D), corresponding to loss of CD8α$^+$ cDCs. Lastly, DCs generated from *Batf3*$^{-/-}$ BM were selectively deficient in Toll-like receptor (TLR) 3-induced interleukin (IL)-12 production (fig. S5C), a specific feature of CD8α$^+$ cDCs (*16*). Similarly, CD11c$^+$ cDCs from the spleens of *Batf3*$^{-/-}$ mice were selectively deficient in TLR3-induced IL-12 production but had normal responses to TLR4 and TLR9 ligands (fig. S6A).

We next tested whether APCs from *Batf3*$^{-/-}$ mice could prime CD4$^+$ and CD8$^+$ T cell responses. Similar proliferative responses of OT-II transgenic CD4$^+$ T cells (*17*) occurred with soluble ovalbumin presented by *Batf3*$^{+/+}$ and *Batf3*$^{-/-}$ cDCs (fig. S6B). However, *Batf3*$^{-/-}$ cDCs were defective in an assay for cross-presentation of cellular antigen to CD8$^+$ T cells (*2*, *18*) (Fig. 3A). OT-I T cells proliferated in response to *Batf3*$^{+/+}$ cDCs cocultured with ovalbumin-loaded cells but failed to proliferate in response to *Batf3*$^{-/-}$ cDCs in this assay.

[1]Department of Pathology and Immunology, Washington University School of Medicine, 660 South Euclid Avenue, St. Louis, MO 63110, USA. [2]Howard Hughes Medical Institute, Washington University School of Medicine, 660 South Euclid Avenue, St. Louis, MO 63110, USA. [3]Departments of Medicine and Molecular Microbiology, 660 South Euclid Avenue, St. Louis, MO 63110, USA.

*To whom correspondence should be addressed. E-mail: kmurphy@wustl.edu

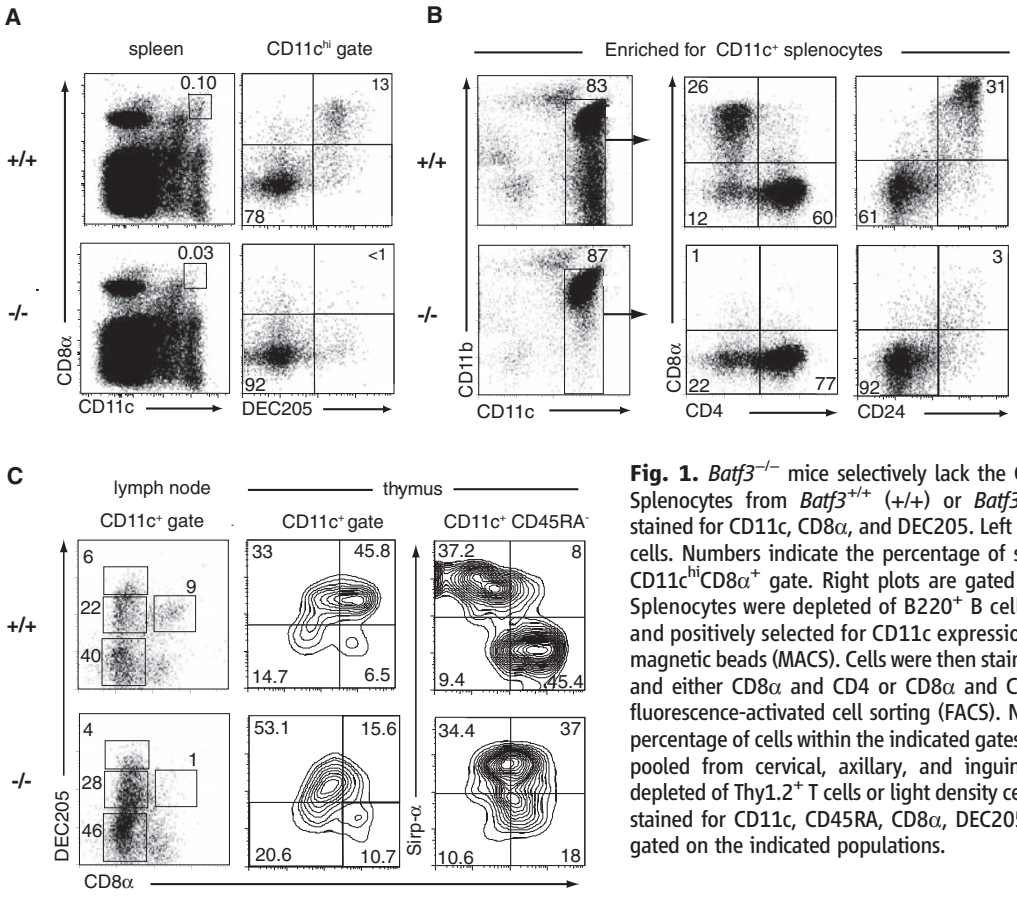

Fig. 1. *Batf3*$^{-/-}$ mice selectively lack the CD8α$^+$ DC subset. (**A**) Splenocytes from *Batf3*$^{+/+}$ (+/+) or *Batf3*$^{-/-}$ (–/–) mice were stained for CD11c, CD8α, and DEC205. Left plots are gated on live cells. Numbers indicate the percentage of splenocytes within the CD11c^{hi}CD8α$^+$ gate. Right plots are gated on CD11c^{hi} cells. (**B**) Splenocytes were depleted of B220$^+$ B cells and Thy1.2$^+$ T cells and positively selected for CD11c expression by antibody-coated magnetic beads (MACS). Cells were then stained for CD11c, CD11b, and either CD8α and CD4 or CD8α and CD24 and analyzed by fluorescence-activated cell sorting (FACS). Numbers represent the percentage of cells within the indicated gates. (**C**) Lymph node cells pooled from cervical, axillary, and inguinal lymph nodes and depleted of Thy1.2$^+$ T cells or light density cells of the thymus were stained for CD11c, CD45RA, CD8α, DEC205, or Sirp-α. Plots are gated on the indicated populations.

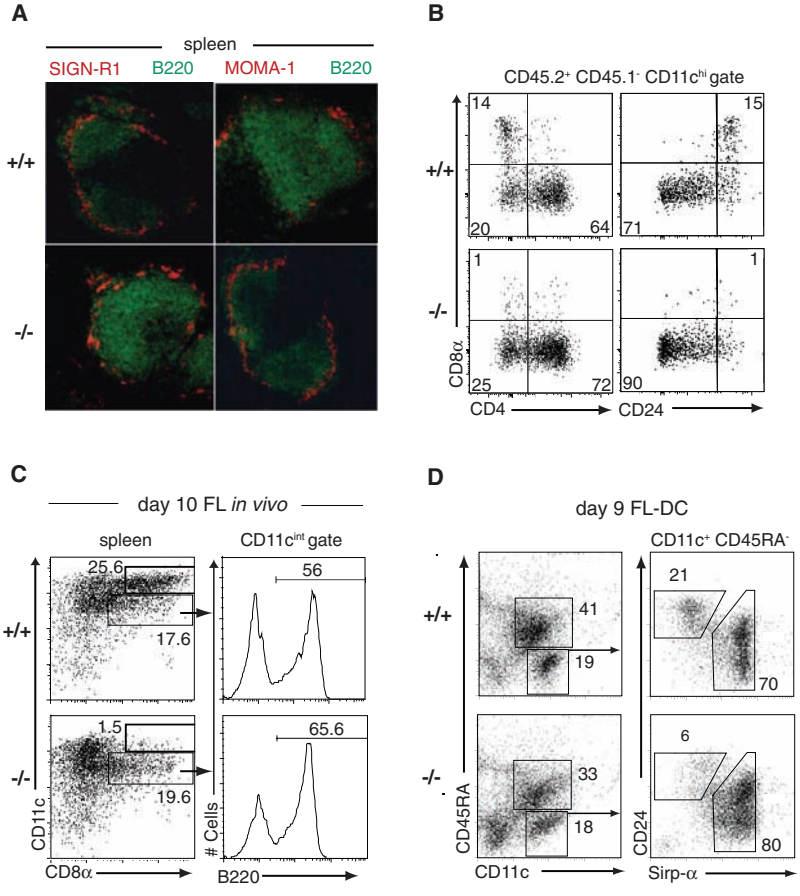

Fig. 2. Functional loss of CD8α$^+$ cDCs in *Batf3*$^{-/-}$ mice is cell-intrinsic to the hematopoietic system. (**A**) Frozen sections from *Batf3*$^{+/+}$ (+/+) or *Batf3*$^{-/-}$ (–/–) mice were stained for B220 (green) and SIGN-R1 (red) expression (left) or for B220 (green) and MOMA-1 (red) (right). (**B**) Irradiated F1(B6.SJL/129SvEv) mice (CD45.1$^+$CD45.2$^+$) were reconstituted with 2 × 10^7 bone marrow cells from *Batf3*$^{+/+}$ (+/+) or *Batf3*$^{-/-}$ (–/–) CD45.1$^-$CD45.2$^+$ mice. After 10 weeks, donor cells (CD45.1$^-$CD45.2$^+$) were analyzed for CD11c, CD8α, CD4, and CD24 expression. Shown are plots for CD8α and CD4 (left) or CD8α and CD24 (right) gated on CD11c^{hi} donor-derived cells. Numbers represent the percentage of cells within the indicated gates. (**C**) *Batf3*$^{+/+}$ (+/+) or *Batf3*$^{-/-}$ (–/–) mice were treated intraperitoneally with 10 μg FL-Fc. After 10 days, splenocytes were enriched for CD11c$^+$ by MACS and stained for CD11c, CD8α, and B220. Plots are gated on live cells (left) or CD11c^{int}CD8α$^+$ cells (right). Numbers represent the percentage of cells within the indicated gates. (**D**) *Batf3*$^{+/+}$ (+/+) or *Batf3*$^{-/-}$ (–/–) BM cells were cultured in FL (20 ng/ml) for 9 days, and nonadherent cells were analyzed for CD11c, CD45RA, CD24, and Sirp-α expression. Plots are gated on live cells (left) or CD11c$^+$ CD45RA$^-$ cells (right).

We examined responses of *Batf3*$^{-/-}$ mice to West Nile virus (WNV) (*19*, *20*) (fig. S6). *Batf3*$^{-/-}$ mice showed normal WNV-specific antibody responses (Fig. 3B) and memory B cell (fig. S6C) and CD4$^+$ T cell responses (fig. S6D) but had a dramatic reduction in WNV-specific CD8$^+$ T cell responses (Fig. 3C) and in vivo cytotoxic T lymphocyte (CTL) killing of WNV peptide–loaded target cells (fig. S7, A and B). *Batf3*$^{-/-}$ mice lacked WNV-specific memory CD8$^+$ T cells and had impaired formation of CD8$^+$CD44^{hi}CD62L^{low} cells (fig. S7). Adoptive transfer of *Batf3*$^{-/-}$ CD8$^+$ T cells into *Rag2*$^{-/-}$ mice generated normal WNV-specific CD8$^+$ T cell response (Fig. 3D), but adoptive transfer of *Batf3*$^{+/+}$ CD8$^+$ T cells into *Batf3*$^{-/-}$ *Rag2*$^{-/-}$ mice generated an impaired WNV-specific CD8$^+$ T cell response (fig. S7C). This shows that impaired WNV-specific CTL responses in *Batf3*$^{-/-}$ mice results from a defect of DCs rather than CD8$^+$ T cells.

We challenged *Batf3*$^{+/+}$ and *Batf3*$^{-/-}$ mice with syngeneic fibrosarcomas that normally are rapidly rejected in a CD4$^+$ and CD8$^+$ T cell–dependent manner (*21*, *22*) (fig. S8A). Two independent fibrosarcomas were rapidly rejected by *Batf3*$^{+/+}$ mice but grew progressively in *Rag2*$^{-/-}$ mice and *Batf3*$^{-/-}$ mice (Fig. 4A and fig. S8, B and C). Moreover, *Batf3*$^{-/-}$ mice failed to develop tumor-specific CTLs (Fig. 4B). Tumor-infiltrating CD8$^+$ T cells, but not CD4$^+$ T cells, were significantly reduced in *Batf3*$^{-/-}$ mice (Fig. 4C). The failure of *Batf3*$^{-/-}$ mice to reject these tumors was not due to defective natural killer cell development or function (figs. S2B and S9, A to C). We considered whether *Batf3*$^{-/-}$ T cells have an intrinsic dysfunction because overexpression studies had suggested *Batf3* might affect IL-2 transcription (*14*). Although *Batf3* overexpression reduces IL-2 reporter activity in Jurkat T cells (fig. S10B), *Batf3*$^{-/-}$ CD4$^+$ T cells showed normal IL-2 production (fig. S10D) and normal T helper cell (T_H) T_H1, T_H2, and T_H17 differentiation (figs. S10, C to E, and S11B). Lastly, *Batf3*$^{-/-}$ CD8$^+$ T cells showed normal allospecific effector responses (fig. S11A) and cytokine production (fig. S11B).

Other DC subsets may cross-present, although less efficiently than CD8α$^+$ DCs (*23*–*26*), suggesting there may be residual cross-presentation capacity in *Batf3*$^{-/-}$ mice. We therefore challenged mice by using reduced tumor-cell numbers, which might allow effective responses in the setting of reduced cross-presentation (fig. S8). Whereas 10^4

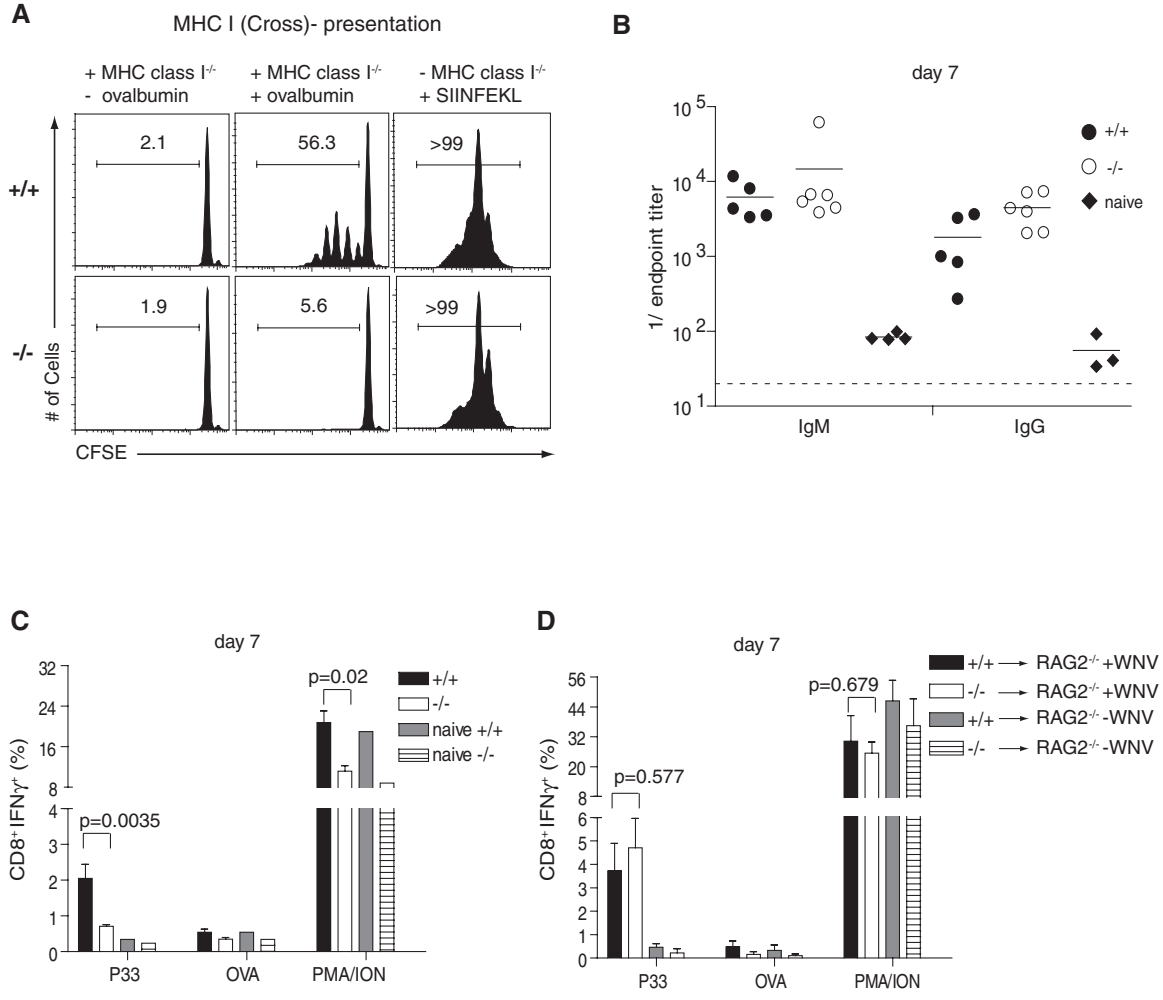

Fig. 3. Lack of cross-presentation and antiviral CTL responses in *Batf3*$^{-/-}$ mice. (**A**) *Batf3*$^{+/+}$ (+/+) or *Batf3*$^{-/-}$ (–/–) splenocytes were depleted of B220$^+$ B cells and Thy1.2$^+$ T cells, enriched for CD11c by MACS, and cultured with irradiated MHC class I$^{-/-}$ splenocytes as indicated that were either untreated (–ovalbumin), pulsed with 10 mg/ml soluble ovalbumin (+ovalbumin), or cultured with 1 μM Ser-Ile-Ile-Asn-Phe-Glu-Lys-Leu (SIINFEKL) peptide. Carboxyfluorescein succinimidyl ester (CFSE)-labeled CD45.1$^+$ OT-I T cells were cultured with these cells, and proliferation was determined by FACS after 60 hours. Single-color histograms of CD8$^+$CD45.1$^+$ OT-I T cells show the percentage of cells in the indicated gates. (**B**) *Batf3*$^{+/+}$ (+/+) or *Batf3*$^{-/-}$ (–/–) mice were infected with 100 plaque-forming units (PFUs) of WNV. On day 7, isotype-specific anti-WNV E protein titers were measured. Horizontal lines represent mean titers and dotted line represents limit of detection. (**C**) *Batf3*$^{+/+}$ (+/+) or *Batf3*$^{-/-}$ (–/–) mice were infected with 100 PFUs of WNV or left uninfected. After 7 days, splenocytes were stimulated in vitro with the WNV-specific NS4B peptide (P33), OVA peptide, or phorbol 12-myristate 13-acetate (PMA)/ionomycin as described. CD8$^+$ T cells were analyzed for expression of intracellular interferon γ (IFN-γ). Data shown are mean ± SEM (n = 9 to 10). (**D**) *Batf3*$^{+/+}$ (+/+) or *Batf3*$^{-/-}$ (–/–) CD8$^+$ T cells were transferred intravenously into *Rag2*$^{-/-}$ recipients. After 24 hours, mice were infected with 100 PFU of WNV (+WNV) or left uninfected (–WNV). After 7 days, splenocytes were harvested and analyzed as described in (C). Data shown are mean ± SEM (n = 6). Three independently performed experiments yielded similar results.

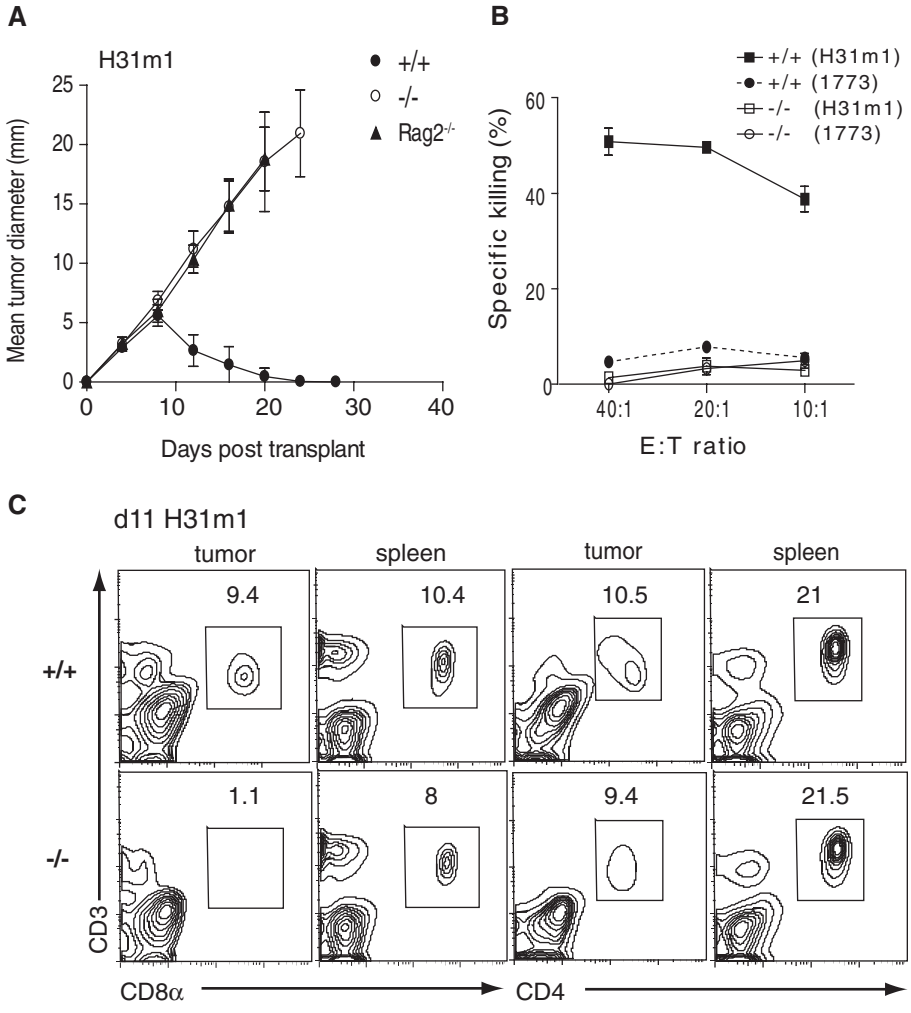

Fig. 4. Lack of tumor rejection in *Batf3*$^{-/-}$ mice. (**A**) 10^6 H31m1 fibrosarcoma cells were injected subcutaneously into *Batf3*$^{+/+}$ (solid circles), *Batf3*$^{-/-}$ (open circles), or *Rag2*$^{-/-}$ (triangles) mice, and tumor diameter (±SD) (n = 10) was measured. (**B**) Mice were treated as in (A). After 9 days, splenocytes were harvested and cocultured with IFN-γ pretreated, irradiated H31m1 tumor cells. After 5 days, a CTL killing assay using ^{51}Cr-labeled H31m1 or 1773 tumor cells as target cells was performed. Shown is specific killing activity as described in (*30*). (**C**) Tumors and spleens from mice treated as in (A) were removed on day 11, and cells analyzed by FACS. Plots are gated on live CD45.2$^+$ cells and show CD3, CD8α, and CD4 expression. Numbers represent the percentage of cells within the indicated gate. Results are representative of at least three mice per group.

and 10^5 tumor cells grew in all *Rag2*$^{-/-}$ mice, some *Batf3*$^{-/-}$ mice controlled this lower tumor burden (fig. S8, D and E) and developed a tumor-specific CTL response (fig. S8F). Whereas adoptive transfer of wild-type DCs led to partial control of tumor growth in *Batf3*$^{-/-}$ mice, transfer of *Batf3*$^{-/-}$ DCs did not (fig. S12).

Subsets of cDCs have recently been described with functional similarities to CD8α$^+$ cDCs. Migratory Langerin$^+$ dermal and lung DC subsets express DEC205$^+$ and CD103$^+$ and, like CD8α$^+$ cDCs, are CD11b$^{lo/-}$ (*27*, *28*). CD8α$^+$ cDC and migratory CD103$^+$ DC populations share the distinctive properties of TLR3 responsiveness (*27*) and capacity for cross-presentation (*26*), further supporting the idea that these CD103$^+$ subsets may be related. In spleen, CD103 is coexpressed with CD8α on cDCs (fig. S13A) (*29*) and selectively expressed by the "CD8α equivalent" CD24$^+$Sirp-α$^{lo\text{-}int}$ cDC subset derived from FL-treated *Batf3*$^{+/+}$ BM (fig. S13C), but is not expressed by *Batf3*$^{-/-}$ splenic cDCs (fig. S13B) or FL-treated *Batf3*$^{-/-}$ BM cells. This suggests that CD103-expressing cDCs may require *Batf3*. In agreement, *Batf3*$^{-/-}$ mice showed a reduced number of CD103-expressing DEC205$^+$CD8α$^-$CD11b$^{lo/-}$ dermal DCs in skin-draining lymph nodes (fig. S14).

This study describes a transcription factor that controls development of CD8α$^+$ cDCs. *Batf3*$^{-/-}$ mice exhibit impaired antigen cross-presentation, impaired CTL responses against viral infection, and impaired responses to tumor challenge. These results suggest an important role for in vivo cross-presentation in CTL responses and provide support for therapeutic approaches that use CD8α$^+$ cDCs for the induction of effective immune responses.

References and Notes

1. M. J. Bevan, *J. Exp. Med.* **143**, 1283 (1976).
2. J. M. den Haan, S. M. Lehar, M. J. Bevan, *J. Exp. Med.* **192**, 1685 (2000).
3. K. Shortman, S. H. Naik, *Nat. Rev. Immunol.* **7**, 19 (2007).
4. R. S. Allan *et al.*, *Science* **301**, 1925 (2003).
5. G. T. Belz *et al.*, *J. Immunol.* **172**, 1996 (2004).
6. G. T. Belz, K. Shortman, M. J. Bevan, W. R. Heath, *J. Immunol.* **175**, 196 (2005).
7. O. Schulz *et al.*, *Nature* **433**, 887 (2005).
8. A. Y. Huang *et al.*, *Science* **264**, 961 (1994).
9. A. F. Ochsenbein *et al.*, *Nature* **411**, 1058 (2001).
10. M. C. Wolkers, G. Stoetter, F. A. Vyth-Dreese, T. N. Schumacher, *J. Immunol.* **167**, 3577 (2001).
11. S. Jung *et al.*, *Immunity* **17**, 211 (2002).
12. H. C. Probst *et al.*, *Clin. Exp. Immunol.* **141**, 398 (2005).
13. M. Zenke, T. Hieronymus, *Trends Immunol.* **27**, 140 (2006).
14. M. Iacobelli, W. Wachsman, K. L. McGuire, *J. Immunol.* **165**, 860 (2000).
15. D. Dudziak *et al.*, *Science* **315**, 107 (2007).
16. S. H. Naik *et al.*, *J. Immunol.* **174**, 6592 (2005).
17. M. J. Barnden, J. Allison, W. R. Heath, F. R. Carbone, *Immunol. Cell Biol.* **76**, 34 (1998).
18. N. S. Wilson *et al.*, *Nat. Immunol.* **7**, 165 (2006).
19. M. S. Diamond, B. Shrestha, A. Marri, D. Mahan, M. Engle, *J. Virol.* **77**, 2578 (2003).
20. E. M. Sitati, M. S. Diamond, *J. Virol.* **80**, 12060 (2006).
21. V. Shankaran *et al.*, *Nature* **410**, 1107 (2001).
22. G. P. Dunn *et al.*, *Nat. Immunol.* **6**, 722 (2005).
23. M. L. Lin, Y. Zhan, J. A. Villadangos, A. M. Lew, *Immunol. Cell Biol.* **86**, 353 (2008).
24. G. T. Belz *et al.*, *Proc. Natl. Acad. Sci. U.S.A.* **101**, 8670 (2004).
25. J. Waithman *et al.*, *J. Immunol.* **179**, 4535 (2007).
26. M. L. del Rio, J. I. Rodriguez-Barbosa, E. Kremmer, R. Forster, *J. Immunol.* **178**, 6861 (2007).
27. S. S. Sung *et al.*, *J. Immunol.* **176**, 2161 (2006).
28. L. S. Bursch *et al.*, *J. Exp. Med.* **204**, 3147 (2007).
29. A. D. Edwards *et al.*, *J. Immunol.* **171**, 47 (2003).
30. Materials and methods are available as supporting material on *Science* Online.

31. This work was supported by the Howard Hughes Medical Institute (K.M.M.), the Emmy Noether Program of the German Research Foundation (K.H.), and a Burroughs Wellcome Fund Career Award for Medical Scientists (B.T.E.).

Supporting Online Material

www.sciencemag.org/cgi/content/full/322/5904/1097/DC1
Materials and Methods
Figs. S1 to S14
References

5 August 2008; accepted 8 October 2008
10.1126/science.1164206